Interfacial Molecular Recognition of Dissolved Thymine by Medium Chain Dialkyl Melamine-Type Monolayers

D. Vollhardt,*,† F. Liu,†,‡ R. Rudert,§ and W. He†,||

Max Planck Institute of Colloids and Interfaces, D-14424 Potsdam/Golm, Germany, Department of Chemistry, Nanjing University, Nanjing 210093, People's Republic China, Federal Institute for Materials Research and Testing, Unter den Eichen 87, D-12200 Berlin, Germany, and State Key Laoratory of Coordination Chemistry, Institute of Coordination Chemistry, Nanjing University, Nanjing 210093, P. R. China

Received: March 1, 2005

Systems consisting of an amphiphilic melamine-type monolayer and a pyrimidine derivative dissolved in the aqueous subphase are good candidates for the formation of interfacial supramolecular assemblies by molecular recognition of hydrogen-bond nonsurface-active species. In the present work, the change in the thermodynamic, phase, and structural properties as a result of molecular recognition of dissolved thymine by 2,4-di(*n*-undecylamino)-6-amino-1,3,5-triazine ($2C_{11}H_{23}$-melamine) monolayers is studied. The combination of surface pressure studies with Brewster angle microscopy (BAM) imaging and grazing incidence X-ray diffraction (GIXD) measurements is optimal for the characterization of the change in structure and phase behavior at the interfacial recognition process. The molecular recognition of the nonsurface-active thymine dissolved in aqueous subphase changes drastically the characteristic features (surface pressure−area isotherms, morphology of the condensed phase domains) of the $2C_{11}H_{23}$-melamine monolayer. It is demonstrated that the kinetics of the recognition process affect largely the main characteristics (phase behavior, morphology of the condensed phase domains) of the interfacial system. The monolayers of $2C_{11}H_{23}$-melamine−thymine assemblies form dumbbell-shaped condensed phase domains not yet observed in other Langmuir monolayers so far. GIXD results show that the molecular recognition of thymine causes only quantitative changes in the two-dimensional lattice structure. Complementary hydrogen bonding of two thymine molecules by one $2C_{11}H_{23}$-melamine molecule is concluded from the chemical structure of both components. Additional information about the nature of the hydrogen bonding on the basis of supramolecular assemblies is obtained by using the quantum chemical PM3 approximation. Energy and lengths of the hydrogen bonds of the optimized thymine−$2C_{11}H_{23}$-melamine−thymine structure are calculated.

Introduction

Molecular recognition processes are of general importance in different fields of biology, chemistry, and physics.[1,2] In the past decade, interfacial molecular recognition and construction of supramolecular assemblies have received considerable attention.[3,4] As is well-known, biological receptors are situated at interfaces of biological systems at which specific molecular recognition processes under decisive participation of hydrogen bonds occur.[5,6] Model systems for molecular recognition between an amphiphilic host-monolayer and a nonsurface-active molecule dissolved in the aqueous subphase can be regarded to be uniquely suited for studying essential features of the supramolecular structures and can help to understand molecular recognition processes at biological interfaces. Hydrogen bond based biomimetic recognition systems have been found effective at the air−water interface.[7−10]

A variety of artificial supramolecular structures has been planned to comprehend molecular recognition by complementary hydrogen bonding. Crystalline architectures have been synthesized.[11] The successful design of supramolecular assemblies by combination of melamine with cyanuric acid or barbituric acid in organic media and in the solid state confirms the high effectiveness of complementary hydrogen bonding.[12−14] Correspondingly, also amphiphilic melamine derivatives have been successfully used as host-monolayers for interfacial molecular recognition. 2,4-Di(*n*-alkylamino)-6-amino-1,3,5-triazine ($2C_nH_{2n+1}$-melamine) monolayers form linear supramolecular networks at the air/water interface at recognition of barbituric acid dissolved in the aqueous subphase.[15,16] In this structure, the hydrogen bonding is linearly extended as both components have two hydrogen binding faces. On the other hand, to our knowledge, interfacial molecular recognition of other pyrimidine derivatives such as thymine, uracil, cytosine, and so forth having only one hydrogen binding face by Langmuir monolayers of the amphiphilic melamine type has not yet been studied. According to the two binding faces of the melamine molecule, it can complementary bind two molecule of these pyrmidine types so that the formation of a linear hydrogen-bonding network can be excluded. It seems reasonable to suppose that such differences in the hydrogen-bonding structure affects also phase behavior and structural features of the supramolecular assemblies formed at interfacial molecular recognition.

Despite the extensive studies of interfacial molecular recognition and numerous direct proofs of guest binding dissolved in the aqueous subphase, to date only little information exists about the changes in the structure and phase properties of the monolayers of the supramolecular structures formed by complementary hydrogen bonding at the air−water interface. Therefore,

* Coresponding author. E-mail: vollh@mpikg-golm.mpg.de.
† Max Planck Institute of Colloids and Interfaces.
‡ Department of Chemistry, Nanjing University.
§ Federal Institute for Materials Research and Testing.
|| Institute of Coordination Chemistry, Nanjing University.

10.1021/jp051036m CCC: $30.25
Published on Web 05/04/2005

we decided to compare the Langmuir monolayers of a selected amphiphilic melamine-type host-molecule with those of the corresponding host−guest assemblies. The present paper focuses on the recognition of thymine by 2,4-di(*n*-undecylamino)-6-amino-1,3,5-triazine ($2C_{11}H_{23}$-melamine) monolayers. A combination of surface pressure studies with Brewster angle microscopy (BAM) imaging and grazing incidence X-ray diffraction (GIXD) measurements has proven to be optimal for the characterization of the change in structure and phase behavior at the interfacial recognition process. Additional information about the nature of the hydrogen bonding based entities can be obtained by quantum chemical calculations. The semiempirical PM3 method is used to optimize the thymine−$C_{11}H_{23}$-melamine−thymine assembly.

Experimental Section

2,4-Di(*n*-undecylamino)-6-amino-1,3,5-triazine ($2C_{11}H_{23}$-melamine) has been selected as host-component for the study of the molecular recognition of a nonsurface-active pyrimidine derivative dissolved in aqueous subphase. The synthesis of the amphiphilic $2C_{11}H_{23}$-melamine was performed according to the scheme

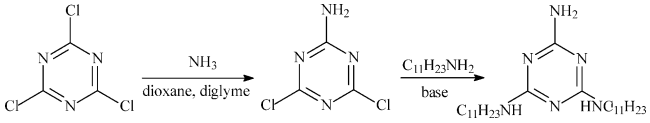

In a first step, 2-amino-4,6-dichloro-1,3,5-triazine was prepared according to ref 12. Ammonia (NH_3) was slowly bubbled into a slurry of cyanuric chloride (36.88 g, 0.2 mol) and diglyme (30 mL) in dioxane (230 mL) cooled in an ice−water bath ($T < 10$ °C). The addition of NH_3 was stopped after ~2 h when 6.8 g (0.4 mol) had been taken up by the mixture. Excess NH_3 was removed by blowing nitrogen through the reaction flask. After filtration, the precipitate was washed well with tetrahydrofurane. The collected solutions were concentrated by rotary evaporation and the solid residue was dried under vacuum yielding 29.5 g of a white powder, mp 218 °C. The obtained 2-amino-4,6-dichloro-1,3,5-triazine was directly used to synthesize the homologous 2,4-di(*n*-alkylamino)-6-amino-1,3,5-triazines ($2C_nH_{2n+1}$-melamine) by aminoalkylation.[17] A mixture of 6 mmol 2-amino-4,6-dichloro-1,3,5-triazine, 12.7 mmol $C_{11}H_{23}NH_2$, and 12.7 mmol $NaHCO_3$ in 100 mL anhydrous dioxane was stirred under reflux for 30 h. The precipitate was removed by filtration and washed with dioxane. After removing the solvent by rotary evaporation, a pale-yellow solid was obtained. Recrystallization in ethanol and heptane resulted in a white final product (purity >99%).

Thymine (purity >97%) obtained from Fluka, Sigma-Aldrich Chemie GmbH was used without further purification. Ultrapure water produced by "Purelab Plus" was used as subphase.

The surface pressure studies were performed in a self-made computer-interfaced film balance equipped with a Wilhelmy balance for the surface pressure determination and a temperature control system.[18] Using a roughened glass plate, the accuracy of the surface pressure was reproducible to ± 0.1 mNm^{-1} and the area per molecule to $\pm 5 \times 10^{-3}$ nm^2. The surface pressure−area ($\pi-A$) isotherms of the amphiphilic melamine-type monolayers spread on pure water and on an aqueous thymine solution were measured at different temperatures and different compression rates in the accessible range.

The morphology of the monolayers was studied using a Brewster angle microscope (BAM 2, NFT, Göttingen) coupled to the film balance. The microscope was equipped with a special scanning technique for providing sharp images. BAM images real in scale and angle were obtained by tilting the CCD sensor of the camera according to the Scheimpflug condition. The application of a green laser (Uniphase, San Jose, CA) allowed a resolution of the BAM images of ~3 μm. More detailed information on the experimental setup and BAM method is given elsewhere; see, for example, refs 18, 19.

The grazing incidence X-ray diffraction (GIXD) experiments were performed using the liquid-surface diffractometer on the undulator beamline BW1 at HASYLAB, DESY, Hamburg, Germany. For reducing the background scattering, the Langmuir trough was placed in a sealed helium-flushed container. The monochromatic synchrotron X-ray beam was adjusted to strike the helium/water interface at a grazing incidence angle $\alpha_i = 0.85\alpha_c$, where α_c is the critical angle for total reflection. The diffracted intensity is detected by a linear position-sensitive detector (PSD) (OED-100-M, Braun, Garching, Germany) as a function of the vertical scattering angle α_f. The detector was rotated around the sample to record the diffracted intensity as a function of the horizontal scattering angle $2\theta_{xy}$. A Soller collimator in front of the PSD restricted the in-plane divergence of the diffracted beam to 0.09 deg. The scattering vector $\mathbf{Q}$ has an in-plane component $\mathbf{Q}_{xy} \approx (4\pi/\lambda)\sin\theta_{xy}$ and an out-of-plane component $\mathbf{Q}_z \approx (2\pi/\lambda)\sin\alpha_f$, where λ is the X-ray wavelength.[20,21] The intensities as a function of $\mathbf{Q}_{xy}$ and $\mathbf{Q}_z$ were least-squares fitted as a Lorentzian in the in-plane direction and as a Gaussian in the out-of-plane direction. The lattice parameters were obtained from the peak positions. The lattice spacing is given by $d(hk) = 2\pi/\mathbf{Q}_{xy}^{hk}$, where (h,k) denotes the order of the reflection. The polar tilt angle t of the long molecule axis and the tilt azimuth ψ_{xy} were calculated from the positions of the $\mathbf{Q}_{xy}$ and $\mathbf{Q}_z$ maxima,[22] according to $\mathbf{Q}_z^{hk} = \mathbf{Q}_{xy}^{hk} \cos\psi_{hk} \tan t$. The lattice parameters a, b, and γ were calculated from the lattice spacing d_{hk} and from these the unit cell area $A_{xy} = ab \sin\gamma$. The cross section per alkyl chain $A_0 = A_{xy} \cos t$ is related to the unit cell area A_{xy} (area per molecule parallel to the interface) and the tilt angle t.

Results and Discussion

At first, we look at the temperature dependence of the experimental $\pi-A$ isotherms of the $2C_{11}H_{23}$-melamine monolayers spread on pure water (Figure 1) and those spread on 0.05 mM and 0.1 mM thymine aqueous subphase (Figures 2 and 3) measured at the same compression rate of 0.04 nm^2/(molecule min). A precondition for the formation of a well-developed two-dimensional domain morphology in Langmuir monolayers is the existence of a plateau region in the $\pi-A$ isotherm within the accessible temperature range that represents the coexistence between a fluid and a condensed phase. This condition is perfectly fulfilled by the $2C_{11}H_{23}$-melamine monolayers. Figure 1 shows eight $\pi-A$ isotherms of $2C_{11}H_{23}$-melamine monolayers in the temperature range between 10.2 and 31.9 °C. It is seen that, over the entire temperature range, at all temperatures a phase coexistence region (plateau) exists, the extension of which decreases clearly as the temperature increases. In this respect, the $2C_{11}H_{23}$-melamine monolayer spread on water behaves as a usual amphiphilic monolayer.[23] At the highest temperature of 31.9 °C, the monolayer collapses at the end of the coexistence region. The phase behavior of the $2C_{11}H_{23}$-melamine monolayer spread on water as well as the thermodynamic characteristics of the transition between the fluid and condensed phase can be obtained from the temperature dependence of phase transition pressure π_c (the kink in the $\pi-A$ isotherms at onset of the phase transition). Figure 1b shows the linear π_c-T relationship of $2C_{11}H_{23}$-melamine spread on water fitted by linear regression.

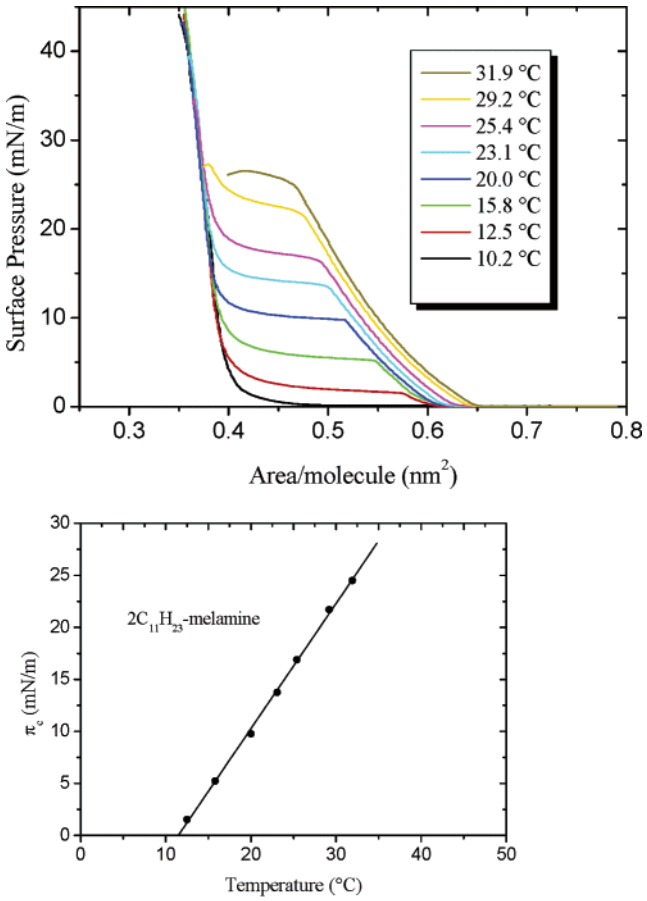

Figure 1. (a) $\pi-A$ isotherms of $2C_{11}H_{23}$-melamine monolayers spread on water measured in the temperature range between 10.2 and 31.9 °C. (b) Temperature dependence of the phase transition pressure π_c of the $2C_{11}H_{23}$-melamine monolayers spread on water.

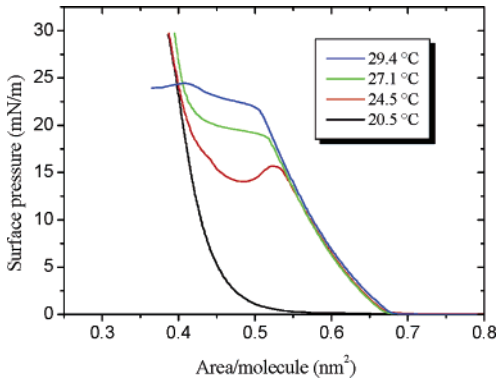

Figure 2. $\pi-A$ curves of $2C_{11}H_{23}$-melamine monolayers spread on 0.05 mM aqueous thymine solution measured in the temperature range between 20.5 and 29.4 °C; compression rate: 0.04 nm²/(min molecule).

Enthalpy, entropy, and free energy for the phase transition of the host-monolayer can be determined from the tilt of the straight $d\pi_c/dT$ line.

Taking into account Traube's rule, Figure 1b indicates that, in the case of $2C_{11}H_{23}$-melamine monolayers, the alkyl chain length is optimal to have the fluid/condensed phase coexistence region in a large accessible temperature range and thus to provide good conditions for studying the domain morphology using Brewster angle microscopy.

The thermodynamic effect of the nonsurface-active thymine dissolved in the aqueous subphase cannot be explained alone by a comparison between the $\pi-A$ isotherms of $2C_{11}H_{23}$-melamine monolayers spread, on one hand, on pure water and, on the other hand, on aqueous thymine solution. Figures 2 and 3 show the $\pi-A$ curves of $2C_{11}H_{23}$-melamine monolayers spread on 0.05 mM and 0.1 mM aqueous thymine solution recorded at the same compression rate of 0.04 nm²/(molecule min) as those spread on water (see Figure 1a). Clear differences between both systems indicate the effect of thymine. In both cases, the plateau for the phase transition is shifted to lower surface pressures at the same temperature. A comparison of Figures 2 and 3 reveals, however, that there are also differences even if the subphase concentration of thymine is not very different. At spreading on 0.05 mM aqueous thymine solution, the plateau disappears at 20.5 °C (Figure 2), in the case of 0.1 mM thymine solution, already at 24.5 °C. Above these temperatures, the $\pi-A$ isotherms show a plateau, but contrary to the isotherms of the $2C_{11}H_{23}$-melamine monolayers spread on water (the behavior of which is generally in agreement with that of usual amphiphilic monolayers), the extension of the plateau increases as the temperature increases. The plateau pressure is reduced the higher the thymine concentration in the subphase. Small surface pressure maxima at the phase transition pressure π_c indicate supersaturation effects.

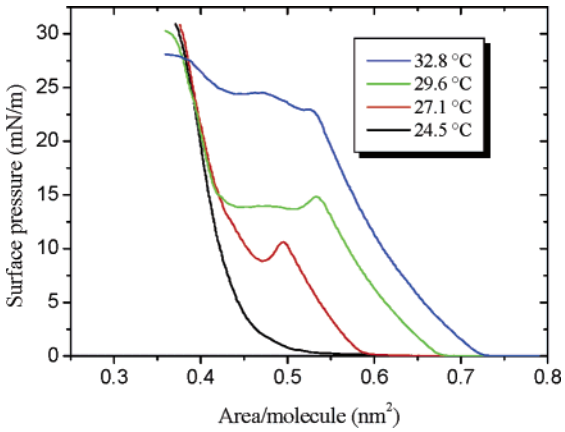

Figure 3. $\pi-A$ curves of $2C_{11}H_{23}$-melamine monolayers spread on 0.1 mM aqueous thymine solution measured in the temperature range between 24.5 and 32.8 °C; compression rate: 0.04 nm²/(min molecule).

However, these unusual features cannot be attributed directly to the development of a new fluid/condensed phase coexistence of adequate supramolecular assemblies. The dependence on the thymine concentration in the subphase suggests that it is rather a matter of the residual material of the host-monolayer that has not yet completely reacted with the dissolved thymine. This is corroborated in a convincing way by recording the $\pi-A$ curves of $2C_{11}H_{23}$-melamine monolayers spread on 0.1 mM thymine solution at different compression rates for $T = 27$ °C (Figure 4). It is seen that the plateau pressure and also the extension of the plateau are largely dependent on the compression rate, and at high velocities, the $\pi-A$ isotherms approach that obtained at spreading on pure water. At low compression rates (0.01 nm²/(molecule min)), the plateau disappears completely. The following conclusions can be drawn from these results. The system achieves equilibrium only at sufficiently slow compression rate. The plateau of the corresponding $\pi-A$ isotherm disappears completely under these conditions. The process of the molecular recognition of the dissolved thymine is completed obviously only in this state. Concerning the bonding kinetics of the dissolved component, equilibrium is reached quicker the higher its concentration. These conclusions are supported by repeated $\pi-A$ compression/decompression curves of $2C_{11}H_{23}$-melamine monolayers spread on 0.1 mM aqueous thymine solution at which large differences between the compression and the decompression curve occur at the first cycle (Figure 5). The

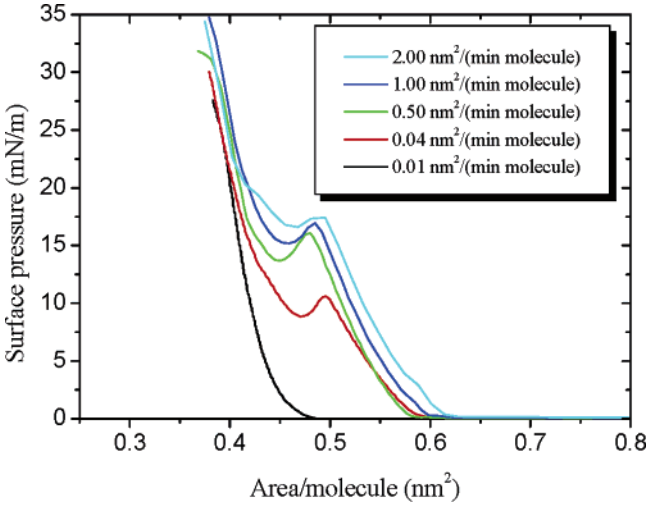

Figure 4. Effect of compression rate on the $\pi-A$ isotherms of $2C_{11}H_{23}$-melamine monolayers spread on 0.1 mM aqueous thymine subphase at 27 °C.

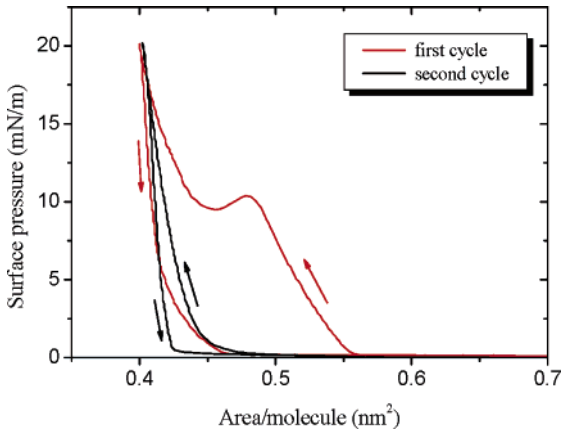

Figure 5. Two repeated $\pi-A$ compression/decompression cycles of $2C_{11}H_{23}$-melamine monolayer spread on 0.1 mM aqueous thymine solution at 27 °C. Large differences exist between the compression and the decompression curve of the first cycle. That difference is small in the second cycle, the isotherms of which resemble the decompression curve of the first cycle.

plateau disappears already in the decompression curve of the first cycle. At renewed cycles, the agreement with the decompression curve remains preserved and a plateau cannot be observed. As expected, the host-$2C_{11}H_{23}$-melamine monolayers spread on water show neither a dependence on the compression rate nor a hysteresis between the $\pi-A$ curves at compression and decompression (not presented in a figure).

Brewster angle microscopy (BAM) is an optimal method to visualize the highly specific changes at the molecular recognition of pyrimidine derivatives by amphiphilic melamine-type monolayers. $2C_{11}H_{23}$-melamine is the best-suitable species of the homologous 2,4-di(*n*-alkylamino)-6-amino-1,3,5-triazines as at the $C_{11}H_{23}$ alkyl chain length the π_c-T dependence indicates the main phase transition over the largest accessible temperature interval (see Figure 1b).

At first, the formation of the condensed phase domains of the $2C_{11}H_{23}$-melamine host-monolayer, spread on water, within the phase coexistence region at 20 °C is illustrated (Figure 6). After the phase transition point π_c at the beginning of the plateau region, numerous small domains are formed (Figure 6, left). At further compression of the monolayer, they grow to essentially larger compact but nontextured domains (middle and

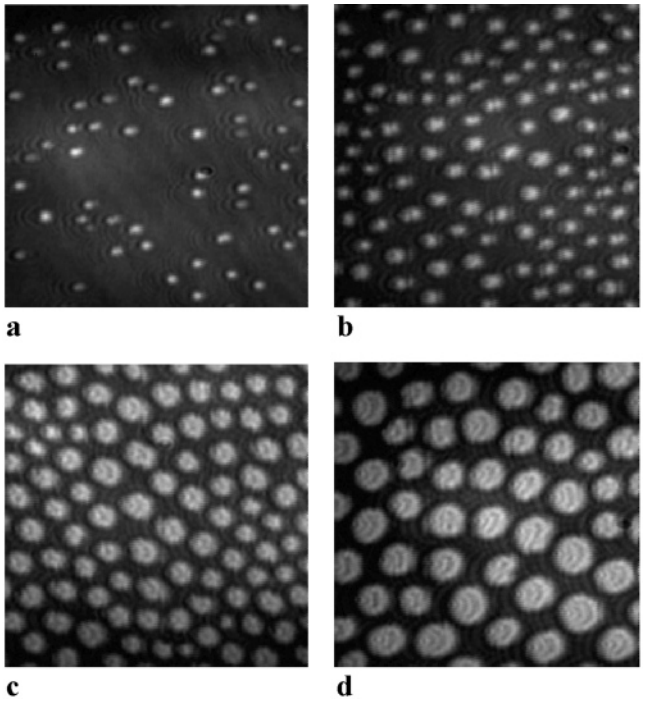

Figure 6. Domain growth within the plateau region of $2C_{11}H_{23}$-melamine monolayer spread on water (from a to d); $T = 20$ °C; image size 400 × 400 mm.

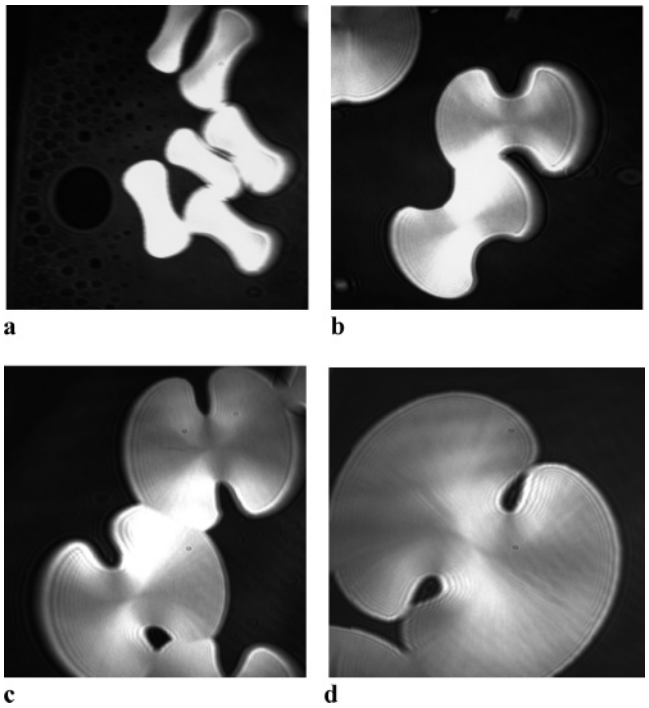

Figure 7. Formation of equilibrium domains of the supramolecular assemblies of $2C_{11}H_{23}$-melamine monolayers spread on 0.1 mM aqueous thymine subphase after compression stop of 30 min at 0.8 nm²/molecule (from a to d); $T = 27$ °C; image size 400 × 400 mm.

right). A modification of temperature has little influence on the shape of the domains.

The morphology of the condensed phase domains changes drastically when the $2C_{11}H_{23}$-melamine monolayer is spread on the aqueous solution of a pyrimidine derivative. Figure 7 shows the domain formation of a $2C_{11}H_{23}$-melamine host-monolayer spread on 0.1 mM thymine solution measured at the compression rate of 0.01 nm²/molecule min and 27 °C. Under these conditions, the molecular recognition process of thymine is

finished and the system is in equilibrium. According to the $\pi-A$ curve obtained at the compression rate of 0.01 nm^2/(molecule min) (see Figure 4), the molecular recognition of the dissolved thymine is completed already at zero pressure. The first small domains are observed at ~0.8 nm^2, that is, the formation of the condensed phase domains starts at zero pressure and a larger area per molecule than that for the onset of the surface pressure increase. The supramolecular entities between $2C_{11}H_{23}$-melamine and thymine form well-developed dumbbell-shaped domains with a specific change of the inner texture. The domains can grow to a considerable size with diameters of ~400 mm. Finally, the two circular segments approach the shape of hemispheres, during which the bar between them is broadened and the segments can touch each other. In the final growth stages, a transition from the dumbbell-like shape to the circular shape seems to be probable.

In most cases, the brightness within the domains changes continuously and also some jumplike changes are observed. The brightness changes represent corresponding changes in the azimuthal long-range orientation of the molecules. Obviously, the orientation changes continuously around the center, or sometimes it jumps at defect lines. Only areas with alkyl chains parallel to the plane of incidence reflect the incident p-polarized light without a change of polarization. The incidence plane is horizontal in the images. This means that the alkyl chains are essentially oriented parallel to the periphery of the two circular segments of the dumbbell-shaped domains. However, the optical anisotropy of the domains is rather weak. This indicates that the alkyl chains are only weakly tilted and thus deviations from the continuous change and irregularities in the long-range orientational order are facilitated.

So far, the formation of dumbbell-shaped domains in Langmuir monolayers has not yet been observed. On the other hand, recently it has been demonstrated that dumbbell-shaped three-dimensional structures have been successfully realized by biomimetic morphogenesis of some minerals (fluorapatite, metal carbonates) by using gelatin and block copolymers as crystal growth modifiers.[24−26] Two-dimensional (2D) simulation has been successfully performed to obtain the unusual dumbbell shape. The simulation started from a 2D needlelike seed and continues with self-similar branching in 5 or 10 successive generations. In the first generation, similar needlelike 2D textures are formed at both ends and have a maximum aperture angle of 45° to the long axis of the seed. A circular segment is formed at both ends of the 2D seed if in each succeeding generation the length of the textures is shorter than the length of the textures of the preceding generation by a certain factor.[24] According to the condition of ref 24, Figure 8 shows the analogous 2D-simulation of a dumbbell-shaped domain for four generations assuming fourfold splitting and a scaledown factor of 0.7 for each new generation.

Additional information on the kinetics of the molecular recognition can be obtained when the compression of the $2C_{11}H_{23}$-melamine monolayer spread on 0.05 mM thymine subphase is stopped before reaching the plateau region of the $\pi-A$ isotherm. The monolayer was compressed with the usually used rate of 0.04 nm^2/(molecule min), stopped at the two different surface pressures of 8.5 mN/m and 13.5 mN/m, and BAM imaging was performed during the $A(t)$ relaxation (Figures 9 and 10). Figure 9b shows some snapshots of the domain development in the course of the $A(t)$ relaxation at $\pi = 8.5$ mN/m for 25 °C. At the constant pressure $A(t)$ relaxation, the A value approximates within <1 h to 0.40 nm^2/molecule (Figure 9a) corresponding to the value of the equilibrium $\pi-A$ isotherm

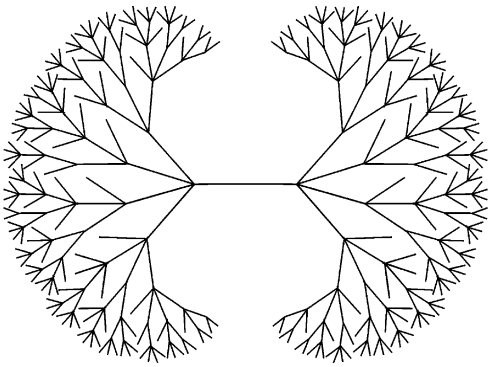

Figure 8. 2D simulation of a dumbbell-shaped domain (barlike seed domain plus four generations) assuming fourfold splitting (with divergence angles of 30°) and a scaledown factor of 0.7 for each new generation. Crossing of the needlelike units is suppressed.

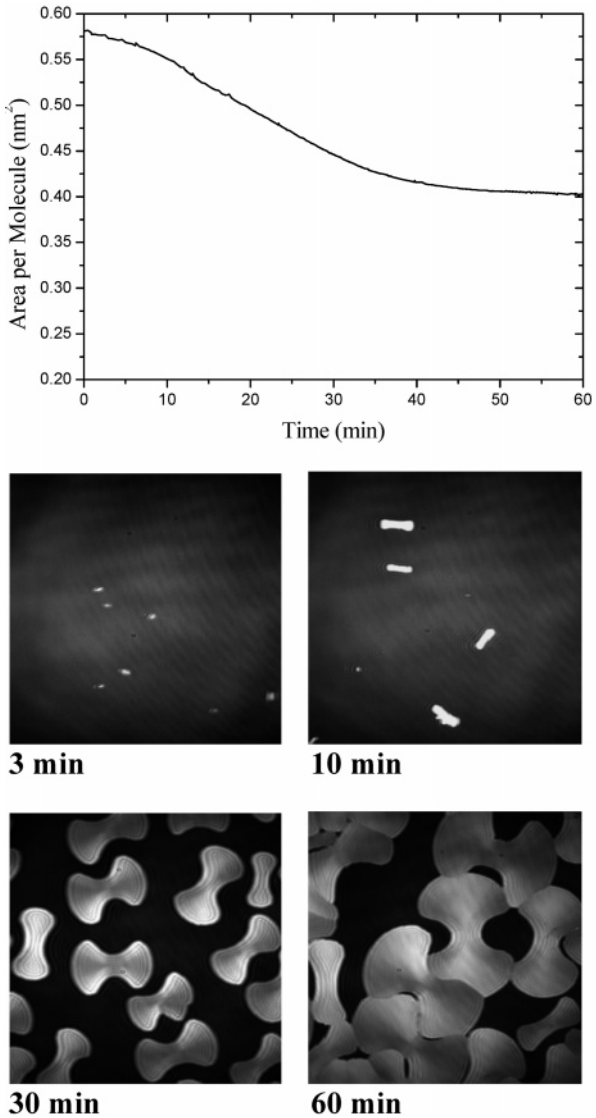

Figure 9. (a) Constant pressure $A(t)$ relaxation (at $\pi = 8.5$ mN/m before reaching the plateau region of the $\pi-A$ isotherm, see Figure 2) of the $2C_{11}H_{23}$-melamine monolayer spread on 0.05 mM thymine subphase; $T = 25$ °C. (b) Domain development in the course of the $A(t)$ relaxation at $\pi = 8.5$ mN/m and 25 °C.

of the supramolecular $2C_{11}H_{23}$-melamine/thymine entity (see Figure 4). The sequence of BAM images of Figure 9b illustrates that, at the beginning of the relaxation process, condensed phase domains are not yet formed. However, already after 3 min the

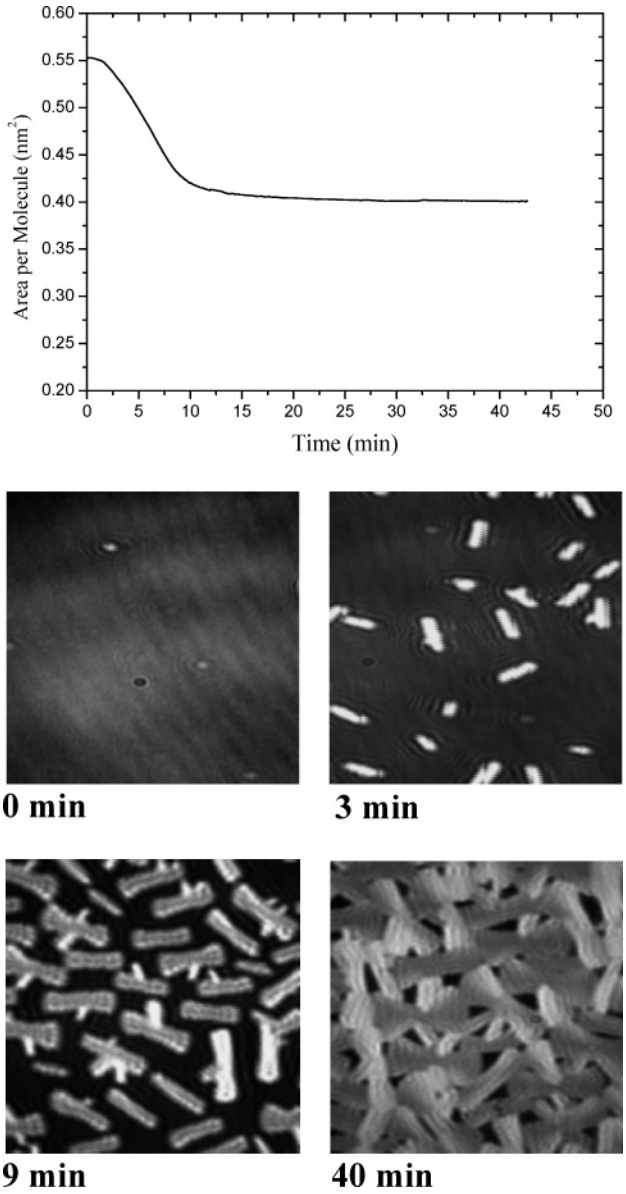

Figure 10. (a) Constant pressure $A(t)$ relaxation (at $\pi = 13.5$ mN/m shortly before reaching the plateau pressure of the $\pi-A$ isotherm, see Figure 2) of the $2C_{11}H_{23}$-melamine monolayer spread on 0.05 mM thymine subphase; $T = 25$ °C. (b) Domain development in the course of the $A(t)$ relaxation at $\pi = 13.5$ mN/m and 25 °C.

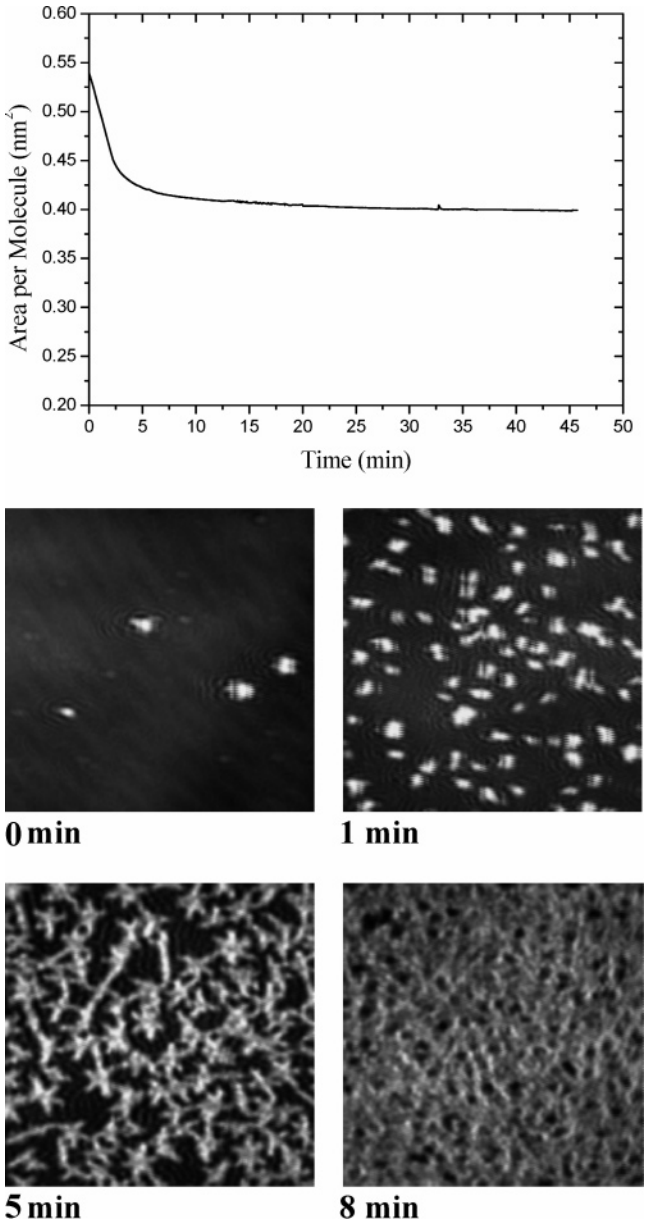

Figure 11. (a) Constant pressure $A(t)$ relaxation (at $\pi = 15.6$ mN/m at the overshoot of the beginning of the plateau region in the corresponding $\pi-A$ curve of the $\pi-A$ isotherm, see Figure 2) of the $2C_{11}H_{23}$-melamine monolayer spread on 0.05 mM thymine subphase; $T = 25$ °C. (b) Development of irregularly shaped domains and, finally, of irregularly dense network of the condensed phase in the course of the $A(t)$ relaxation at $\pi = 15.6$ mN/m and 25 °C. The formation of regularly formed condensed phase domains is obviously disturbed by the presence of the first nuclei of pure $2C_{11}H_{23}$-melamine monolayer material.

first small seed domains can be observed. At 10 min, these seeds are grown to small domains of a barlike shape. It is seen that the process of broadening starts at the end of the barlike domain. The image taken after 30 min shows well-developed dumbbell-shaped domains that are grown to larger size and overlap partially after 60 min. The growth stages of the $2C_{11}H_{23}$-melamine−thymine domains during the $A(t)$ relaxation at $\pi = 8.5$ mN/m demonstrated in Figure 9b are in agreement with the results of the 2D simulation of dumbbell-shaped textures starting with a needle texture in the first generation.

Figure 10 shows the domain development when the $A(t)$ relaxation is studied at $\pi = 13.5$ mN/m, that is, the compression of the monolayer is stopped shortly before reaching the plateau pressure (see Figure 2). Here, the process of constant pressure $A(t)$ relaxation and thus the kinetics of the molecular recognition go much quicker, as seen in Figure 10a. Again, at the beginning, condensed phase domains cannot be observed. The sequence of BAM images (Figure 10b) shows that, after 3 min, numerous bar-shaped domains are formed. According to the quicker process of thymine recognition, the nucleation rate for the $2C_{11}H_{23}$-melamine−thymine domains is much higher. Correspondingly, the number of domains increases rapidly with time. After 9 min, numerous small domains are formed which are slightly broadened at both ends of the bars and thus they resemble the shape of dumbbells. Because of the competition between nucleation rate and growth rate, a further growth is largely limited, so that finally after 40 min a mixture of numerous small domains are observed overlapping each other.

However, the situation changes generally when, under the same compression conditions as before, the $A(t)$ relaxation is performed at the slightly higher surface pressure $\pi = 15.6$ mN/m at the overshoot of the beginning of the plateau region in the corresponding $\pi-A$ curve, seen in Figure 2. Here, most of the

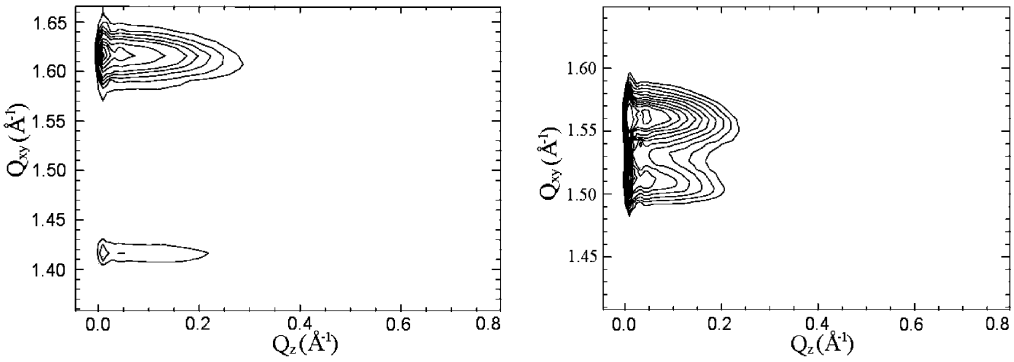

Figure 12. GIXD contour plots of the corrected diffraction intensities as a function of the in-plane ($\mathbf{Q}_{xy}$) and out-of-plane ($\mathbf{Q}_z$) components of the scattering vectors for a $2C_{14}H_{29}$-melamine monolayer spread on water (left) and on 0.1 mM thymine subphase (right); $T = 20$ °C; $\pi = 20$ mN/m.

TABLE 1

Lattice Parameters for $C_{14}H_{29}$-Melamine on Pure Water at 20 °C							
surface pressure (mN/m)	a (nm)	b (nm)	A_{xy} (nm^2)	A_0 (nm^2)	t (deg)	γ (deg)	tilt direction
1	0.444	0.498	0.1979	0.1968	6.1	116.5	NNN
10	0.443	0.497	0.1970	0.1962	5.3	116.5	NNN
20	0.442	0.496	0.1964	0.1958	4.5	116.4	NNN
30	0.439	0.494	0.1943	0.1940	3.5	116.4	NNN
Lattice parameters for $C_{14}H_{29}$-Melamine on 0.1 mM Thymine at 20 °C							
surface pressure (mN/m)	a (nm)	b (nm)	A_{xy} (nm^2)	A_0 (nm^2)	t (deg)	γ (deg)	tilt direction
1	0.462	0.479	0.1939	0.1938	1.3	118.8	NNN
10	0.461	0.476	0.1921	0.1921	1.3	118.9	NNN
20	0.460	0.476	0.1917	0.1917	1.2	118.9	NNN
23	0.460	0.476	0.1917	0.1917	0.8	118.9	NNN

relaxation takes place already within the first 5 min (Figure 11a). The corresponding domain development is demonstrated in Figure 11b. The first condensed phase domains appear already at the beginning, the number of which increases considerably within the first minute. After 5 min, the domains touch each other and start to coalesce. Already after 8 min, an irregularly dense network of the condensed phase is formed. Generally, the domain size is small and the shape largely irregular. The tendency to form the irregular shapes observed is obviously a consequence of the fact that the plateau of the corresponding $\pi-A$ curve indicates the phase transition of the $2C_{11}H_{23}$-melamine monolayer, the material of which has not yet recognized the dissolved thymine molecules. First nuclei of pure $2C_{11}H_{23}$-melamine monolayer material affect and disturb the formation of regularly formed condensed phase domains of the supramolecular $2C_{11}H_{23}$-melamine−thymine structures.

GIXD studies provide additional information on the structure of the condensed phase at the formation of the supramolecular entities. The question arises whether and in which way the alkyl chain lattice structure of the pure host-monolayer is affected by the formation of the supramolecular assemblies after molecular recognition of the guest-component dissolved in aqueous subphase. This can be qualitatively demonstrated by a comparison of the adequate contour plots seen in the number and position of the reflexes. As a representative example, Figure 12 shows the comparison of the contour plots of the corrected diffraction intensities as a function of the in-plane ($\mathbf{Q}_{xy}$) and out-of-plane ($\mathbf{Q}_z$) components of the scattering vector for the $2C_{14}H_{29}$-melamine monolayer spread on water (left-hand side) and that obtained after molecular recognition of thymine dissolved in the aqueous subphase at 20 °C. In both cases, the position of the two reflexes at $\mathbf{Q}_z > 0$ (despite the small distance from zero) indicates a centered-rectangular lattice with tilt of the alkyl chains in direction of next nearest neighbors (NNN). It is, however, clearly seen that the molecular recognition of thymine gives rise only to quantitative change in the structure of the rectangular lattice. The characteristic lattice data of $2C_{14}H_{29}$-melamine monolayer spread on water and spread on aqueous thymine solution are listed in Table 1 for different surface pressures. The polar tilt angle t is already small at low surface pressures and decreases further as the surface pressure increases. The polar tilt angle is even smaller after molecular recognition of thymine and approximates to zero, that means, to nearly perpendicular orientation. The lattice parameters a and b are almost equal so that the deviation from the hexagonal structure is small.

The chemical structure of 2,4-di(*n*-undecylamino)-6-amino-1,3,5-triazine ($2C_{11}H_{23}$-melamine) reveals two binding faces on both sides of the headgroup whereas the dissolved thymine has only one binding face. Therefore, complementary hydrogen bonding of two thymine molecules by one $2C_{11}H_{23}$-melamine molecule should be expected by the interfacial molecular recognition. The chemical structure of the formed supramolecular assembly is shown in Figure 13. Quantum chemical calculations provide additional information about the nature of the hydrogen bonding based assemblies. The semiempirical PM3 method[27] was used to create and to optimize models of $2C_{11}H_{23}$-melamine and thymine. For $2C_{11}H_{23}$-melamine, a conformer with nearly parallel alkyl chains and relatively low energy was chosen because the alkyl chains in a condensed surface layer are usually densely packed and aligned parallel to each other. According to the structure of the supramolecular entity discussed above, the hydrogen-bonding energy between one $2C_{11}H_{23}$-melamine molecule and two thymine molecules was calculated as follows. The geometries of the three hydrogen-bonded molecules were optimized (Figure 14), then the energy of the supramolecular assembly was calculated, and finally the sums of the calculated energies of the two isolated thymine molecules and the hydrogen-bonded $2C_{11}H_{23}$-melamine−thymine pair were subtracted (see Table 2). The differences (−32.1/−32.5 kJ/mol)

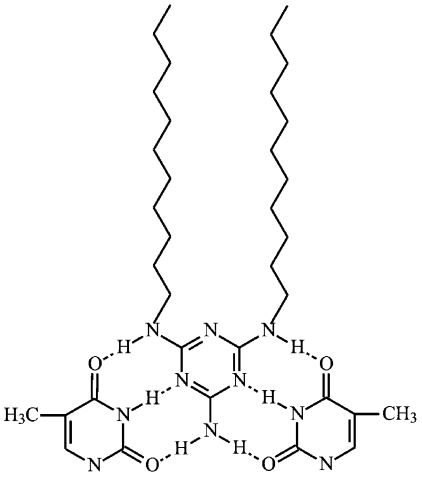

Figure 13. Chemical structure of the supramolecular assembly between 2,4-di(*n*-undecylamino)-6-amino-1,3,5-triazine ($2C_{11}H_{23}$-melamine) and thymine formed at the interface.

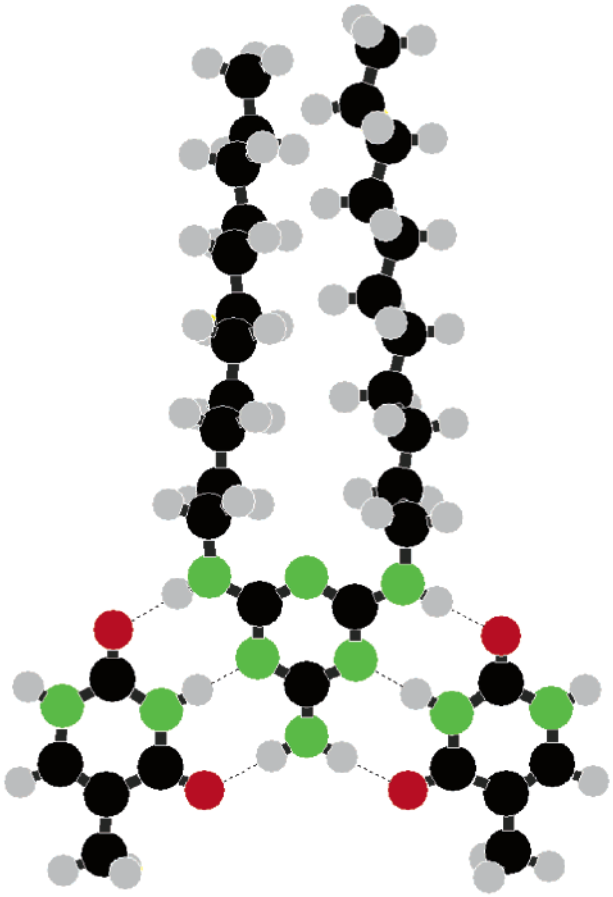

Figure 14. Geometry of the PM3-optimized thymine−$2C_{11}H_{23}$-melamine−thymine complex.

TABLE 2

molecules	PM3 energy [kJ/mol]
thymine−$2C_{11}H_{23}$-melamine−thymine	−45381.22
thymine (2)	−6648.76/−6648.71
thymine−$2C_{11}H_{23}$-melamine	−38700.34/−38699.97

represent the hydrogen-bonding energy of one binding face of $2C_{11}H_{23}$-melamine and thymine. These high-energy values which are only slightly dependent on the molecular conformation express the high stability of the supramolecular structure. The corresponding energies of the two thymine molecules are not exactly the same because the conformation of $2C_{11}H_{23}$-melamine is not completely symmetric. The lengths of the hydrogen bonds are 0.185−0.186 nm for O···H and 0.174 nm for H···N.

Conclusions

So far, comprehensive studies of interfacial molecular recognition and numerous direct proofs of guest binding dissolved in the aqueous subphase substantiate the current interest in this subject. However, there has been little information about the structure and phase properties of the monolayers of the supramolecular assemblies formed by complementary hydrogen bonding at the air−water interface. The present work should be a contribution to fill this gap. Langmuir monolayers of a selected amphiphilic melamine-type host-molecule 2,4-di-(*n*-undecylamino)-6-amino-1,3,5-triazine ($2C_{11}H_{23}$-melamine) and those of the corresponding supramolecular entity with dissolved nonsurface-active thymine are systematically compared. The combination of surface pressure studies with Brewster angle microscopy (BAM) imaging and grazing incidence X-ray diffraction (GIXD) measurements has proven to be optimal for the characterization of the changes in structure and phase behavior at the interfacial recognition process. The characteristic features ($\pi-A$ isotherms, phase behavior, morphology of the condensed phase domains) of the $2C_{11}H_{23}$-melamine monolayers are drastically changed by molecular recognition of the nonsurface-active thymine dissolved in aqueous subphase. However, molecular recognition of thymine gives rise only to quantitative differences in the structure of the rectangular lattice with tilt of the alkyl chains in NNN direction formed by both the pure $2C_{11}H_{23}$-melamine monolayer and the $2C_{11}H_{23}$-melamine−thymine entity. The analysis of the experimental results reveals a large effect of the kinetics of the recognition process on the main characteristics (phase behavior, morphology of the condensed phase domains) of the interfacial system. Pure $2C_{11}H_{23}$-melamine monolayers form nontextured compact domains whereas the monolayers of the $2C_{11}H_{23}$-melamine−thymine entities form dumbbell-shaped condensed phase domains not yet observed in other Langmuir monolayers so far. 2D simulation can be successfully performed to obtain the unusual dumbbell shape demonstrated after starting with a barlike seed domain for four generations, assuming fourfold splitting and a scaledown factor of 0.7 for each new generation.

Complementary hydrogen bonding of two thymine molecules by one $2C_{11}H_{23}$-melamine molecule is concluded from the chemical structure of both components. The melamine headgroup has two binding faces on both sides of the triazine ring whereas the thymine molecule has only one binding face. Additional information about the nature of the hydrogen bonding based supramolecular structures can be obtained by using the quantum chemical PM3 approximation. The high-energy value of the complementary hydrogen bonds of the optimized thymine−$2C_{11}H_{23}$-melamine−thymine structure corroborates the results of the main characteristics.

Acknowledgment. Financial support from the Deutsche Forschungsgemeinschaft (DFG grant VO-710/ 7-1) is gratefully acknowledged.

References and Notes

(1) Lehn, J.-M. *Angew. Chem., Int. Ed. Engl.* **1990**, *29*, 1304.
(2) Philip. D.; Stoddart, J. F. *Angew. Chem., Int. Ed. Engl.* **1996**, *35*, 1154.
(3) Kunitake, T. *Thin Solid Films* **1996**, *284/285*, 9.
(4) Ariga, K.; Kunitake, T. *Acc. Chem. Res.* **1998**, *31*, 371 and refs therein.

(5) Alberts, B.; Bray, D.; Lewis, J.; Raff, M.; Roberts, K.; Watson, J. D. *Molecular Biology of the Cell*, 2nd ed.; Garland Publishing: New York, 1989.
(6) Wenz, G. *Angew. Chem., Int. Ed. Engl.* **1994**, *33*, 803.
(7) Bohanon, T. M.; Denzinger, S.; Fink, R.; Paulus, W.; Ringsdorf, H.; Weck, M. *Angew. Chem., Int. Ed. Engl.* **1995**, *34*, 58.
(8) Shimomura, M.; Nakamura, F.; Ijiro, K.; Taketsuna, H.; Tanaka, M.; Nakamura, H.; Hasebe, K. *J. Am. Chem. Soc.* **1997**, *119*, 2341.
(9) Sasaki, D. Y.; Kurihara, K.; Kunitake, T. *J. Am. Chem. Soc.* **1992**, *114*, 10994.
(10) Taguchi, K.; Ariga, K.; Kunitake, T. *Chem. Lett.* **1995**, 701.
(11) Desiraju, G. R. *Angew. Chem.* **1995**, *107*, 2541.
(12) Zerkowski, J. A.; MacDonald, J. C.; Seto, C. T.; Wierda, D. A.; Whitesides, G. M. *J. Am. Chem. Soc.* **1994**, *116*, 2382.
(13) Zerkowski, J. A.; Whitesides, G. M. *J. Am. Chem. Soc.* **1994**, *116*, 4298.
(14) Zerkowski, J. A.; Mathias, J. P.; Whitesides, G. M. *J. Am. Chem. Soc.* **1994**, *116*, 4305.
(15) Ebara, Y.; Itakura, K.; Okahata, Y. *Langmuir* **1996**, *12*, 5165.
(16) Matsuura, K.; Ebara, Y.; Okahata, Y. *Langmuir* **1997**, *13*, 814.
(17) Koyano, H.; Bissel, P.; Yoshihara, K.; Ariga, K.; Kunitake, T. *Chem. Eur. J.* **1997**, *3*, 1077.
(18) Vollhardt, D. *Adv. Colloid Interface Sci.* **1996**, *64*, 143.
(19) Meunier, J. *Colloids Surf., A* **2000**, *171*, 33.
(20) Als-Nielsen, J.; Jacquemain, D.; Kjaer, K.; Leveiller, F.; Lahav, M.; Leiserowitz, L. *Phys. Rep.* **1994**, *246*, 251.
(21) Kjaer, K. *Physica B* **1994**, *198*, 100.
(22) Als-Nielsen, J.; Kjaer, K. In *Phase Transitions in Soft Condensed Matter*; Riste, T., Sherrington, D., Eds.; NATO ASI Series B; Plenum Press: New York, 1989; Vol. 211, p 113.
(23) Fainerman, V. B.; Vollhardt, D. *J. Phys. Chem. B* **1999**, *103*, 145.
(24) Kniep, R.; Busch, S. *Angew. Chem., Int. Ed. Engl.* **1996**, *35*, 2624.
(25) Busch, S.; Dolhaine, H.; DuChesne, A.; Heinz, S.; Hochrein, O.; Laeri, F.; Podebrad, O.; Vietze, U.; Weiland, T.; Kniep, R. *Eur. J. Inorg. Chem.* **1999**, 1643.
(26) Yu, S.-H.; Cölfen, H.; Antonietti, M. *J. Phys. Chem. B* **2003**, *107*, 7396.
(27) Stewart, J. J. P. *J. Comput. Chem.* **1989**, *10*, 221.